INTO THE WILD: A JOURNEY TO CHAOS IN FOUR DIMENSIONS

Juan Patiño-Echeverría, Hinke Osinga and Bernd Krauskopf

Department of Mathematics, University of Auckland

The unpredictable nature of chaos

Why do we often need a raincoat when the forecast promises sunshine? Why do some mathematical models seem to predict the future better than others? The meteorologist Edward Lorenz found that the problem was unpredictability; to explain it, he introduced the concept of ***chaos***.

Overview

Different forms of chaos exist in higher dimensions. We study the 4D Lorenz-like system:

$$\begin{cases} \dot{x} = \sigma\,(y - x), \\ \dot{y} = \rho\, x - y - x\, z, \\ \dot{z} = x\, y - \beta\, z + \mu\, w, \\ \dot{w} = \quad -\mu\, z - \beta\, w, \end{cases}$$

which has a ***wild chaotic attractor*** according to [1] for the values $\beta = 8/3, \sigma = 10, \rho = 25$ and $\mu = 7$; see Figure 1.

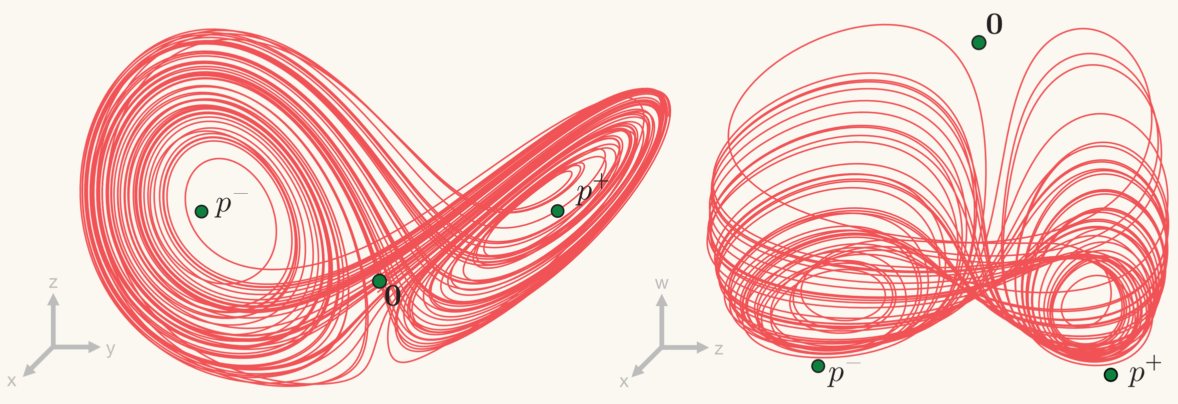

Figure 1. Projections of the wild chaotic attractor onto (x, y, z)-space (left) and onto (x, z, w)-space (right) with the equilibria $\mathbf{0}$ and $p^{\pm}$ (green dots).

- What is the difference between this wild chaotic attractor and a classical chaotic attractor?
- Why these parameter values?
- What invariant sets are involved in creating wild chaos?

We want to answer these questions by using a geometric approach to study qualitative changes in the dynamics as ρ and μ vary.

Bifurcation Diagram

We first construct the two-parameter bifurcation diagram of the 4D system, starting from the bifurcation points of the classic Lorenz system. This construction is achieved by finding bifurcation curves in the (ρ, μ)-plane for fixed $\beta = 8/3$ and $\sigma = 10$, with the continuation software AUTO [2]. Figure 2 shows the curves P of pitchfork, H of Hopf, T of torus, PD of period-doubling, F of cyclic folds, EtoP of equilibrium to periodic orbit, and Hom_r of (basic) homoclinic bifurcation.

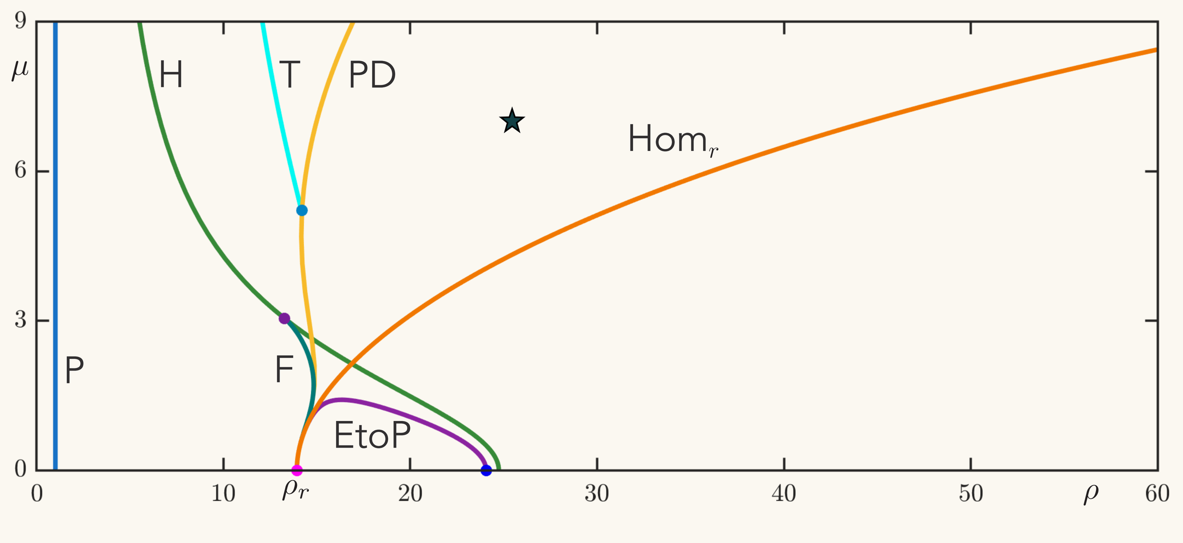

Figure 2. The basic two-parameter bifurcation diagram of the 4D Lorenz-like system in the (ρ, μ)-plane. The star at $(25, 7)$ is where the wild chaotic attractor exists, according to [1].

The homoclinic orbits to the origin are of chaotic Shilnikov type for $\mu > 0$. Figure 3 shows projections of the Shilnikov homoclinic orbit on the curve Hom_r at $\mu = 4$ and $\rho \approx 23.8$.

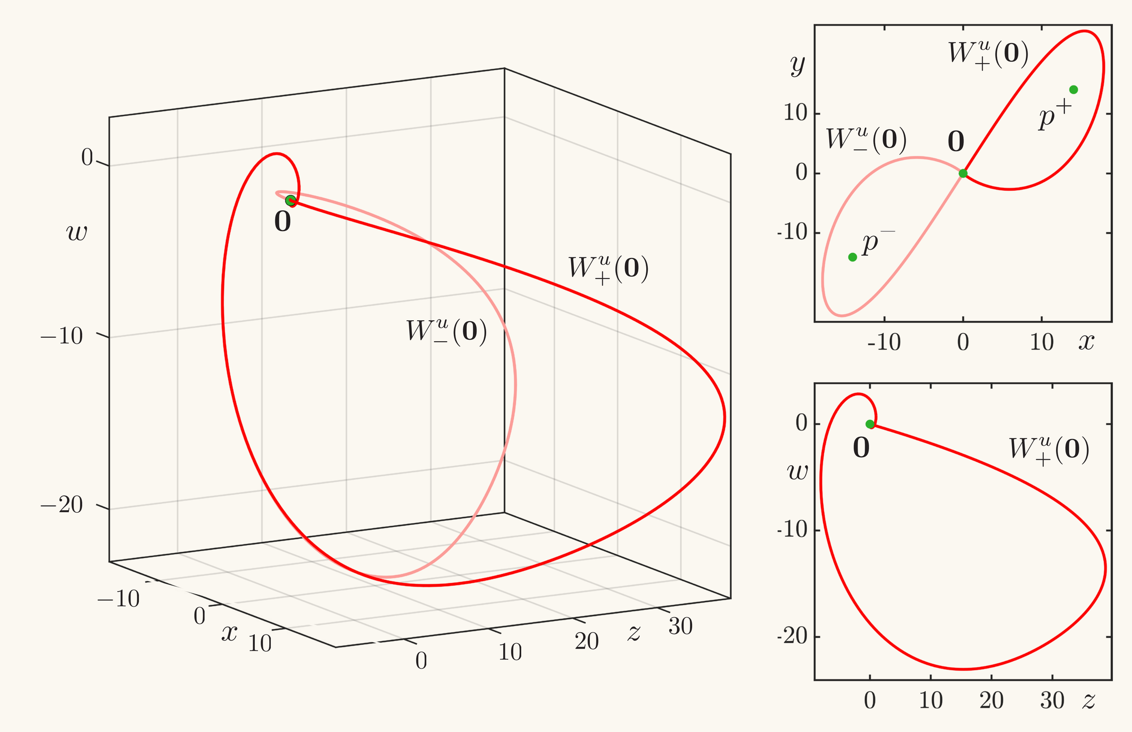

Figure 3. Spiralling near the origin illustrates the Shilnikov-type nature of the basic homoclinic orbit to $\mathbf{0}$, formed by the branches $W^u_+(\mathbf{0})$ (dark red) and $W^u_-(\mathbf{0})$ (light red) of the unstable manifold of the origin.

Different homoclinic bifurcations

To study the entire parameter (ρ, μ)-plane, we compactify it to the unit square with the transformation $(\tilde{\rho}, \tilde{\mu}) = (\rho/(25+\rho), \mu/(7+\mu))$. Figure 4 shows the resulting bifurcation diagram with curves of additional homoclinic bifurcations that also exist in the classic Lorenz system [3].

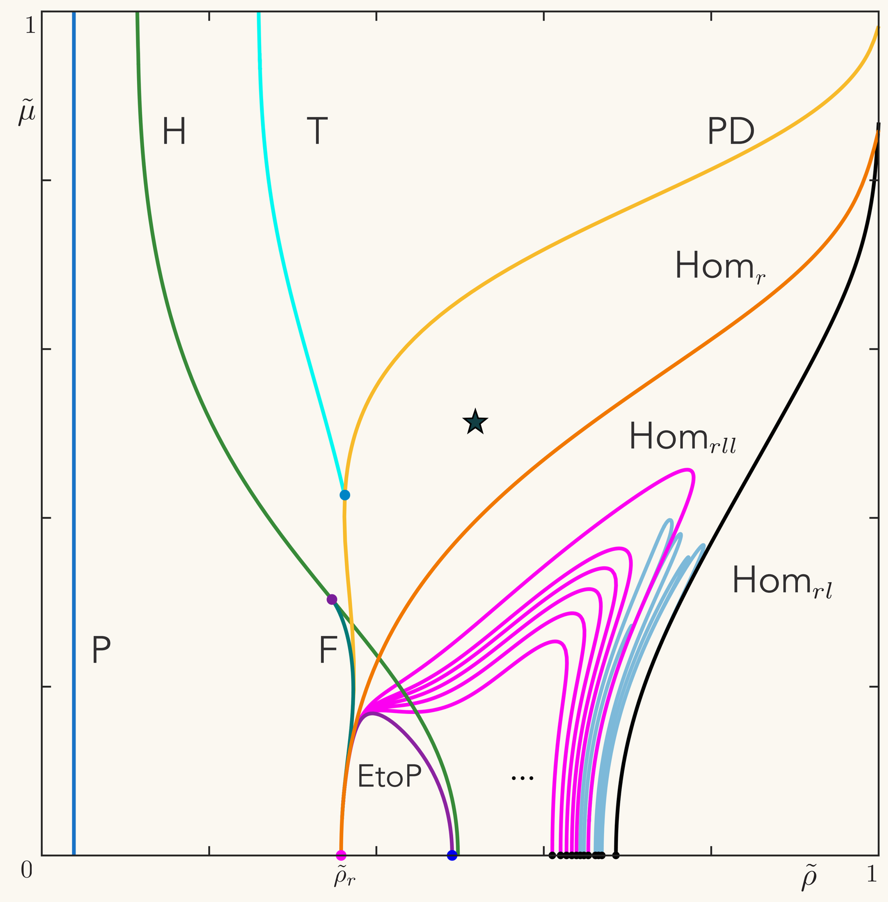

Figure 4. Two-parameter bifurcation diagram of the 4D Lorenz-like system in the compactified $(\tilde{\rho}, \tilde{\mu})$-square. The bifurcation curves from Figure 2 are shown with additional curves of homoclinic bifurcations of different signatures (grey and light blue).

The different homoclinic bifurcations make excursions around the equilibria $p^{\pm}$, which define their signatures; see Figure 5. Note that the curve of EtoP ends at $\tilde{\rho}_r$ on the $\tilde{\rho}$-axis; see Figure 6.

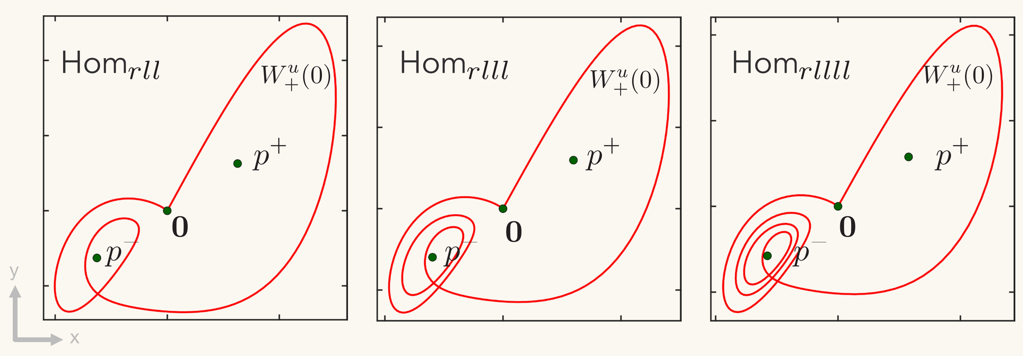

Figure 5. Homoclinic orbits of different signatures in projection onto the (x, y)-plane.

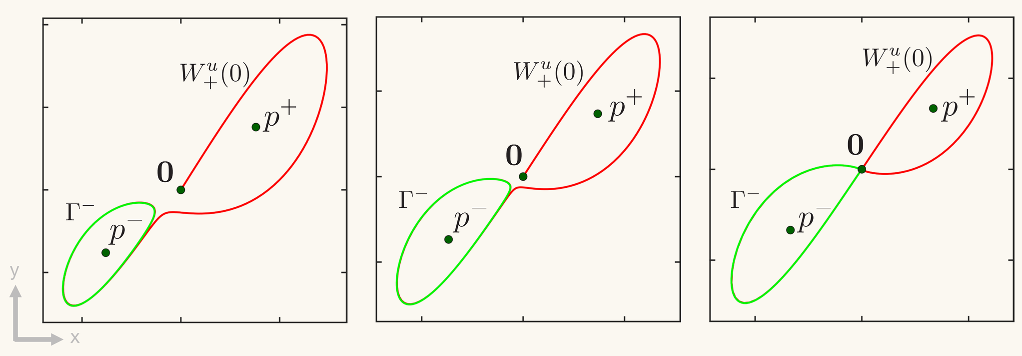

Figure 6. Connecting orbits in projection onto the (x, y)-plane as the point $\tilde{\rho}_r$ is approached along the curve EtoP from Figure 4.

Kneading diagram

We construct a kneading diagram [4] from the branch $W^u_+(\mathbf{0})$ that defines the signature by assigning a sequence of + and – depending on whether $W^u_+(\mathbf{0})$ goes around p^+or p^-, respectively.

View from the (x, y)-plane	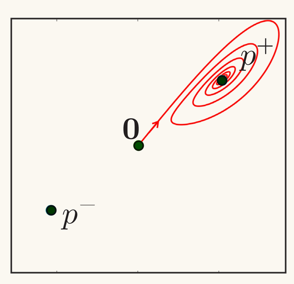	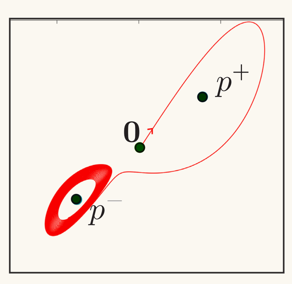
Sequence	$(++++\ldots)$	$(+---\ldots)$

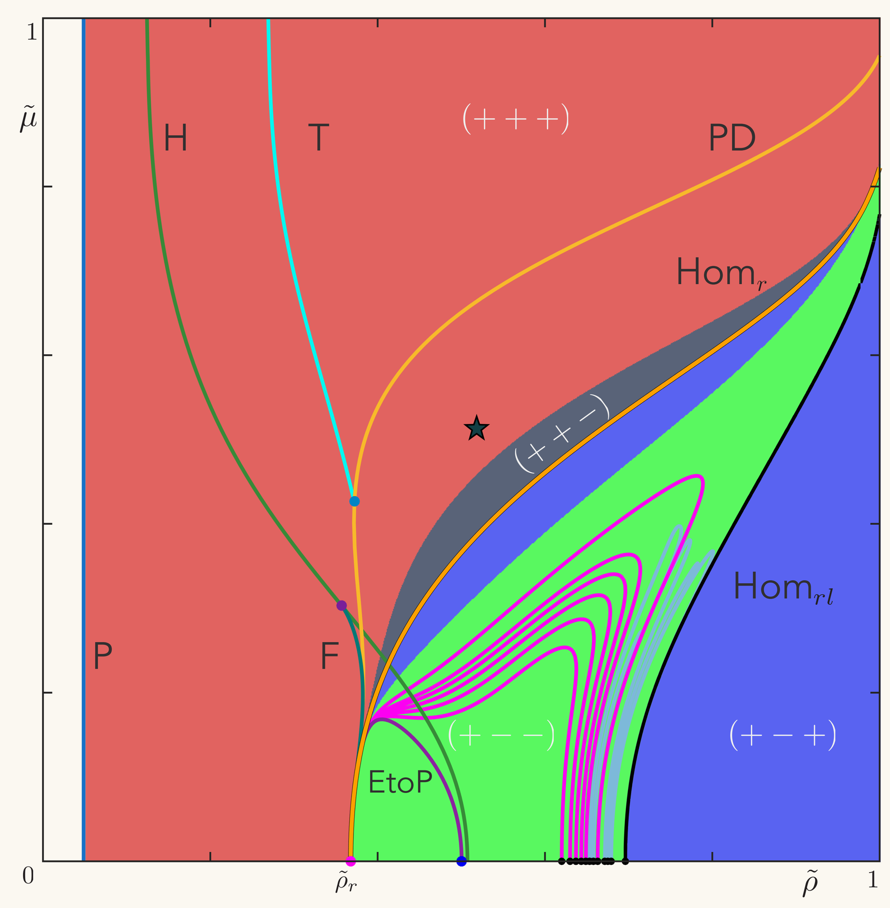

Figure 7. Kneading diagram of three symbols of $W^u_+(0)$ together with the bifurcation curves of Figure 4.

Results

- The EtoP bifurcation is not directly responsible for creating the wild chaotic attractor.
- The homoclinic explosion point $(\rho_r, 0)$ acts as an organising centre; from it emerges local and global bifurcations.
- There are new homoclinic bifurcations of different signatures that are not present in the classic Lorenz system.

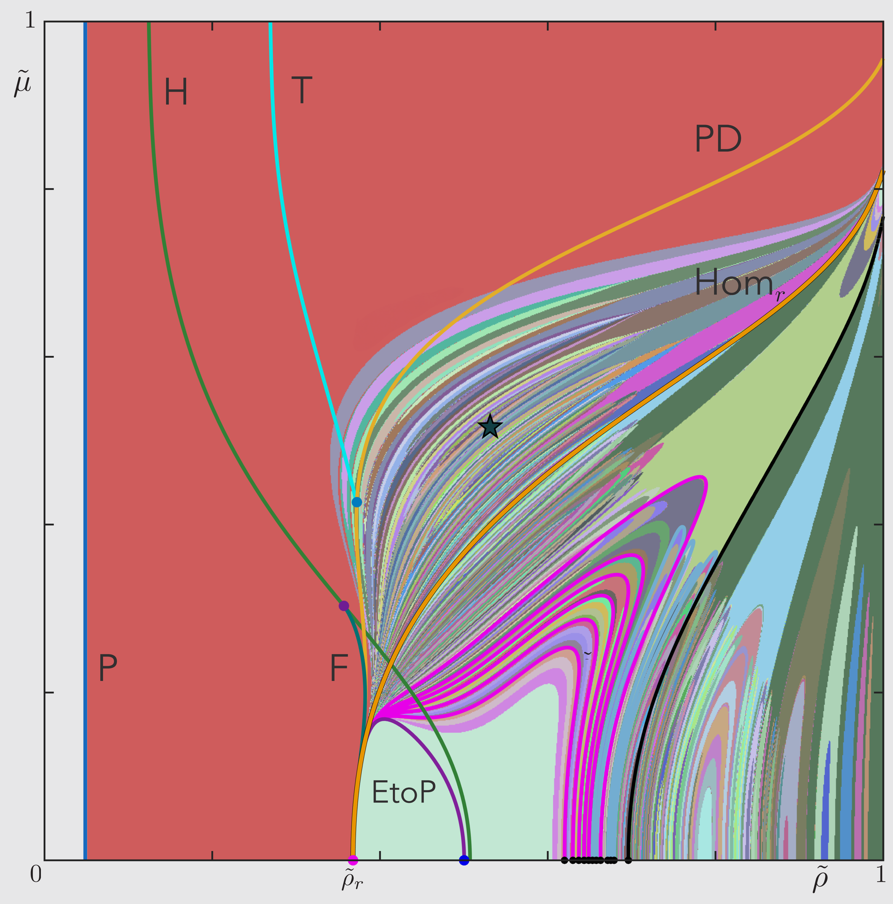

Figure 8. Kneading diagram of eight symbols of $W^u_+(0)$ together with the bifurcation curves of Figure 4.

Ongoing work

- Characterising other global bifurcations from the kneading diagram of more symbols.
- Studying the exact relationship between the bifurcation structure and the Lyapunov spectrum.

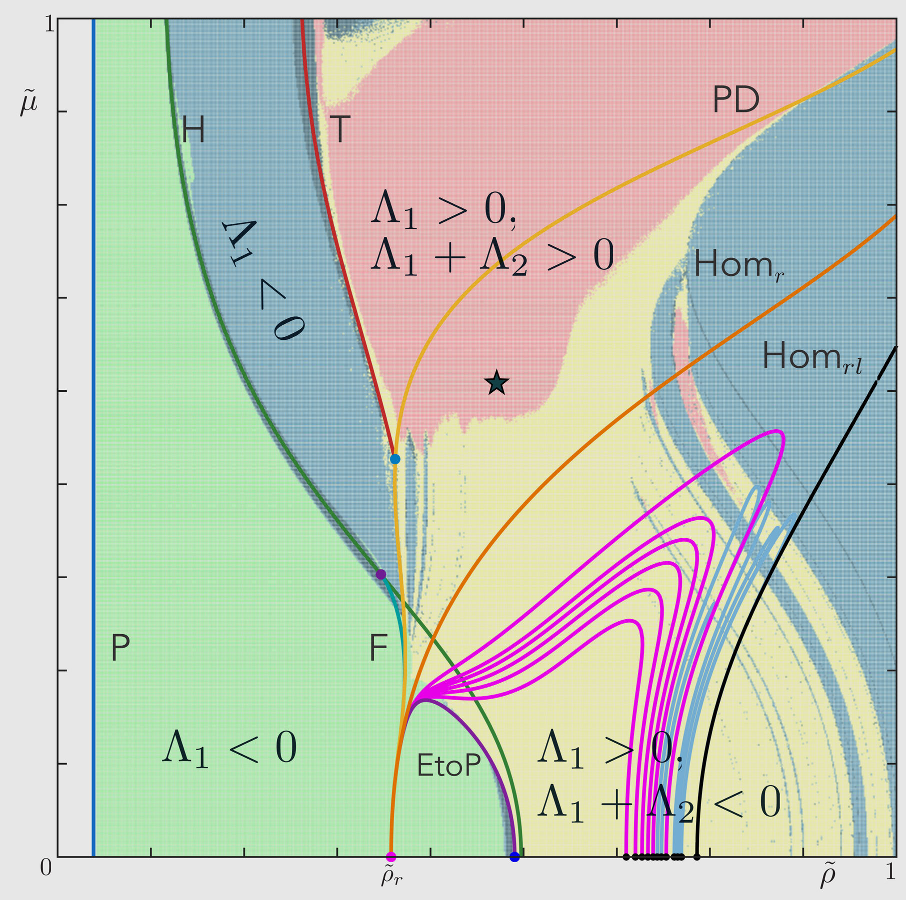

Figure 9. Lyapunov spectrum together with the bifurcation curves of Figure 4. The regime with $\Lambda_1 > 0,\ \Lambda_1 + \Lambda_2 > 0$ is conjectured to feature wild chaos.

References

1. Gonchenko, S., Kazakov, A., & Turaev, D. (2021). Wild pseudohyperbolic attractor in a four dimensional Lorenz system. Nonlinearity, 34: 2018-2047.
2. Doedel, E., Oldeman, et al.(2007). AUTO-07p: Software for continuation and bifurcation problems in ordinary differential equations. Retrieved from http://indy.cs.concordia.ca/auto/.
3. Doedel, E. J., Krauskopf, B., & Osinga, H. M. (2006). Global bifurcations of the Lorenz manifold. Nonlinearity, 19: 2947-2972.
4. Barrio, R., Shilnikov, A., & Shilnikov, L. P. (2012). Kneadings, symbolic dynamics and painting Lorenz chaos. International Journal of Bifurcation and Chaos. 22. 1230016.

Contact

Juan Patiño-Echeverría
j.patino@auckland.ac.nz